

# Visualization of doxorubicin-induced oxidative stress in isolated cardiac myocytes

NARINE SARVAZYAN

Department of Physiology, Texas Tech University Health Sciences Center, Lubbock, Texas 79430

**Sarvazyan, Narine.** Visualization of doxorubicin-induced oxidative stress in isolated cardiac myocytes. *Am. J. Physiol.* 271 (*Heart Circ. Physiol.* 40): H2079–H2085, 1996.—The paper presents high-resolution fluorescence images obtained using laser-scanning confocal microscopy. Isolated cells from adult rat hearts were preloaded with 2',7'-dichlorofluorescein (an oxidant-sensitive fluorescent probe) and exposed to doxorubicin, an important anticancer drug with prominent cardiotoxicity. Fluorescence images were collected from live cells simultaneously on two channels: 1) 515–530 nm emission range was used to monitor an increase in dichlorofluorescein, the oxidized product of dichlorofluorescein, and 2) emission >610 nm was used to visualize the intracellular distribution of doxorubicin. The images reveal intracellular oxidation close to the mitochondria after only 20 min of exposure of isolated cardiomyocytes to 40–160  $\mu\text{M}$  doxorubicin. The data confirm an oxidative mechanism of doxorubicin cardiotoxicity and demonstrate the capability of a new technique to monitor intracellular oxidation in living cardiomyocytes.

oxygen free radicals; confocal microscopy; dichlorofluorescein; cardiomyocytes

THE RANGE of pathophysiological and physiological phenomena that implicate reactive oxygen species as culprits of injury or as secondary messengers continues to expand. Today they include apoptosis, ischemia-reperfusion injury, aging, inflammation, neuromuscular diseases, cancer, atherosclerosis, regulation of vascular tone, and many other phenomena (2, 11, 20). However, the assortment of methods that can noninvasively assess oxygen reactive metabolites in vivo remains rather limited (21). The most frequently used electron spin resonance technique is prone to several artifacts and is unable to assess subcellular patterns of oxygen free radicals (17, 21). Therefore, the development of techniques that are capable of monitoring oxidative stress associated with specific subcellular sites is in great demand. One of those new techniques is high spatial and temporal resolution laser-scanning confocal microscopy combined with oxidant-sensitive fluorescent probes (20). The present study contributes to the development of this new approach by revealing oxidative stress associated with doxorubicin exposure in isolated cardiac myocytes.

Doxorubicin is an anthracycline antibiotic that is used for treatment of a wide range of human neoplasms. Unfortunately, its application is associated with an acute as well as cumulative dose-related cardiomyopathy (6, 18). Several mechanisms have been suggested to explain the cardiotoxicity of doxorubicin: formation of free radicals (14, 18), changes in cardiac muscle gene expression (10), sensitization of  $\text{Ca}^{2+}$  release from sarcoplasmic reticulum channel (19), and alteration of mitochondrial membrane function (3). The

free radical-based mechanism of doxorubicin is supported by many studies (13, 14, 18), including our earlier study which revealed that cardiomyocytes with a diminished level of superoxide dismutase are more susceptible to doxorubicin exposure (23). The major criticism of the oxidative mechanism of doxorubicin action is that the majority of evidence favoring this hypothesis of doxorubicin cardiotoxicity has been obtained by studying subcellular fractions, often in combination with extremely high concentrations of doxorubicin not encountered in clinical practice (16, 18). The present study demonstrates that 1) an increase in intracellular oxidation after brief exposure to doxorubicin can be directly visualized in isolated cardiac cells, 2) elevated oxidation levels are observed in close proximity to the mitochondria, and 3) accumulated concentrations of doxorubicin in mitochondria of live cardiomyocytes can be two orders of magnitude higher than the actual concentration of the drug in the media.

## MATERIALS AND METHODS

**Preparation of cardiomyocytes.** Two-month-old Sprague-Dawley rats (200–300 g) were injected with heparin sodium (500 U/kg ip). After 20–25 min the rats were anesthetized with pentobarbital sodium (45 mg/kg ip). The excised hearts were perfused for 10 min with Joklik's modified minimum essential medium (MEM) supplemented with 1.25 mM  $\text{CaCl}_2$ , perfused for 5 min with a nominally  $\text{Ca}^{2+}$ -free MEM supplemented with 20 mM creatine and 60 mM taurine, and perfused for 6–10 min with the same medium containing 0.5–1 mg/ml of type II collagenase and 0.1% bovine serum albumin (BSA). The ventricles were then minced and vigorously shaken in the same medium containing 2% BSA. After two washes in collagenase-free medium, the  $\text{CaCl}_2$  concentration in the medium was gradually increased to 1.25 mM. With this method,  $5\text{--}7 \times 10^6$   $\text{Ca}^{2+}$ -tolerant cells per heart were routinely obtained (percentage of myocytes retaining rod-shaped morphology was 65–70% of the total cell numbers, whereas percentage of unstained cells was ~80%). Myocyte viability was evaluated by microscopic determination of the number of rod-shaped cells and the number of myocytes that excluded trypan blue (24).

**Cell loading with fluorescent probes.** A 10 mM stock solution of 2',7'-dichlorofluorescein diacetate (DFDA) was prepared in ethanol on a daily basis and diluted to a final concentration of 10  $\mu\text{M}$  just before the experiments. A single batch of DFDA was used in all experiments. After intracellular deacetylation, DFDA forms a nonfluorescent product (dichlorofluorescein), which upon oxidation is transformed into highly fluorescent dichlorofluorescein (28). Myocytes were preincubated with 10  $\mu\text{M}$  DFDA for 40 min in MEM containing 1.25 mM  $\text{CaCl}_2$ , 1% BSA, and 25 mM *N*-2-hydroxyethylpiperazine-*N'*-2-ethanesulfonic acid (HEPES, pH 7.3). To verify specific sites of intracellular doxorubicin distribution (doxorubicin is a highly fluorescent compound, see below), the cells were also stained with rhodamine-123, a well-known mitochondrial marker (25). Doxorubicin-treated myocytes were



incubated with 1  $\mu\text{M}$  rhodamine-123 for 2 min and subsequently washed twice to remove the excess dye.

**Fluorescence measurements.** Cells were observed through a Plan-Apo  $\times 100$  (NA 1.4) oil-immersion objective on an inverted Olympus microscope with an Olympus LSM GB200 confocal imaging system attached. Excitation of dichlorofluorescein and doxorubicin was achieved using the 488-nm line of a 15-mW argon-ion laser attenuated to 1% intensity. Use of a low-intensity laser in the scanning mode should have minimized photooxidation of the probe as well as other artifacts associated with exposure of the cell to the laser beam (20). Nevertheless, continuous illumination of cells loaded with DFDA, even with the low-intensity laser beam (0.15-mW total intensity), slowly increased dye fluorescence. To avoid these photooxidation artifacts, the following approach was used: the observation field was quickly (2 s/scan) scanned once to localize the cells, and a final high-resolution image was obtained by a single scanning (40 s/scan). The emitted light was collected simultaneously on two optical channels. *Channel I* was equipped with two emission filters, 515-nm long pass and  $510 \pm 20$ -nm band pass, that, in combination, selected emitted light in the 515- to 530-nm range. *Channel I* detected dichlorofluorescein emission and therefore reflected changes in oxidation. *Channel II* was equipped with a 610-nm long-pass filter and was used for doxorubicin imaging. The same filters set for *channels I* and *II* were used for dual staining with rhodamine-123 and doxorubicin. Emission spectra for doxorubicin and dichlorofluorescein were obtained using a Delta Scan spectrofluorometer (Photon Technology). Dichlorofluorescein was obtained by hydrolysis and subsequent oxidation of DFDA by hydrogen peroxide (22).

**Incubation with doxorubicin.** For short-term treatment, myocytes ( $1 \times 10^4$  cells/ml) were incubated with doxorubicin (40–160  $\mu\text{M}$ ) in Tyrode solution supplemented with 25 mM HEPES (pH 7.3) for 20 min. Incubations were done directly in the chamber used for subsequent microscopic observations. For long-term treatment, myocytes ( $1 \times 10^4$  cells/ml) were incubated for 20 h in MEM containing 1  $\mu\text{M}$  doxorubicin, 25 mM HEPES (pH 7.3), and 100  $\mu\text{g/ml}$  gentamicin. Five microliters of cell suspension were then transferred to 200  $\mu\text{l}$  of Tyrode solution for acquisition of the images.

**Image acquisition and analysis.** Variation of acquisition parameters drastically changes the appearance of confocal images, either obscuring or emphasizing the observed effects. Specifically, those parameters include size of the pinhole (which determines the field of the depth from which the emission image is collected), intensity of the excitation beam, speed of the scanning, and photomultiplier tube settings for each acquisition channel (voltage, gain, and offset). Thus, to provide a valid comparison, exactly the same settings were used for control and doxorubicin-exposed samples. To reveal the pattern of doxorubicin accumulation after long-term exposure, the pinhole size on *channel II* was increased to the maximum (8 mm), and the other settings were kept the same. All images were collected at room temperature. The images were analyzed with Olympus LSM GB200 software. Line intensity analysis function was used on two channels simultaneously to confirm mitochondrial localization of doxorubicin. Mean fluorescence intensity was calculated by averaging area intensities from a number of outlined cells. For each condition described, four to seven images of different cells were collected. A similar number of observations were made for the cells treated with doxorubicin alone and DFDA alone. Myocyte images were saved as TIFF files and pseudocolored using NIH Image software.

**Materials.** Collagenase II was obtained from Worthington (Freehold, NJ). Doxorubicin, MEM, gentamicin, albumin, and HEPES were purchased from Sigma Chemical (St. Louis, MO). DFDA and rhodamine-123 were obtained from Molecular Probes (Eugene, OR).

## RESULTS

**Dual staining of live cardiomyocytes with doxorubicin and dichlorofluorescein.** Emission spectra of dichlorofluorescein and doxorubicin allowed separation of the fluorescence from cells stained simultaneously with both ionophores (Fig. 1). Loading with DFDA caused a slight increase in the intensity of the cell image on *channel I* without affecting *channel II*. Exposure of DFDA-loaded cells to 100  $\mu\text{M}$  hydrogen peroxide resulted in intense intracellular oxidation; this dramatically increased the fluorescence signal on *channel I* without affecting an image on *channel II*. Although a small portion of the doxorubicin emission spectra overlapped with *channel I*, cells treated with doxorubicin alone exhibited on *channel I* less than 2% of the intensity detected on *channel II*. Thus the selected settings for *channels I* and *II* provided adequate separation of dichlorofluorescein and doxorubicin fluorescence, allowing assessment of intracellular oxidation in cells exposed to doxorubicin.

Another aspect that needs to be considered is possible quenching of dichlorofluorescein fluorescence by doxorubicin, because there is a partial spectral overlap between two probes (27). However, this effect would underestimate, rather than overestimate, the true dichlorofluorescein production at high doxorubicin concentrations, whereas sensitivity of this approach to detect free radical formation at low drug concentrations would not be altered.

**Intracellular accumulation of doxorubicin.** In the present study, doxorubicin concentrations ranged from 40 to 160  $\mu\text{M}$ . As shown previously (23), such concentrations do not affect cardiomyocyte viability when exposure is less than 30 min. Because intracellular oxidation was assessed after 20 min of exposure to doxorubicin, it was important to verify the presence

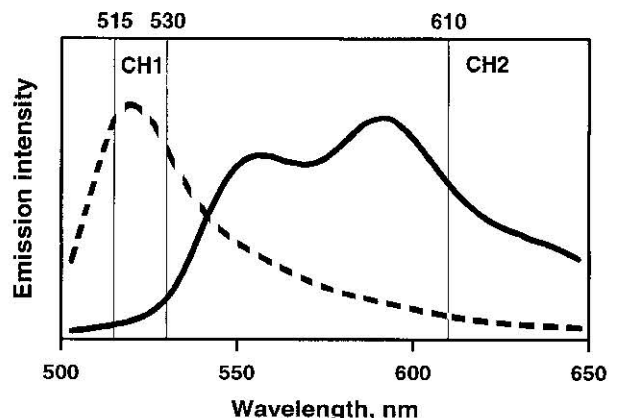
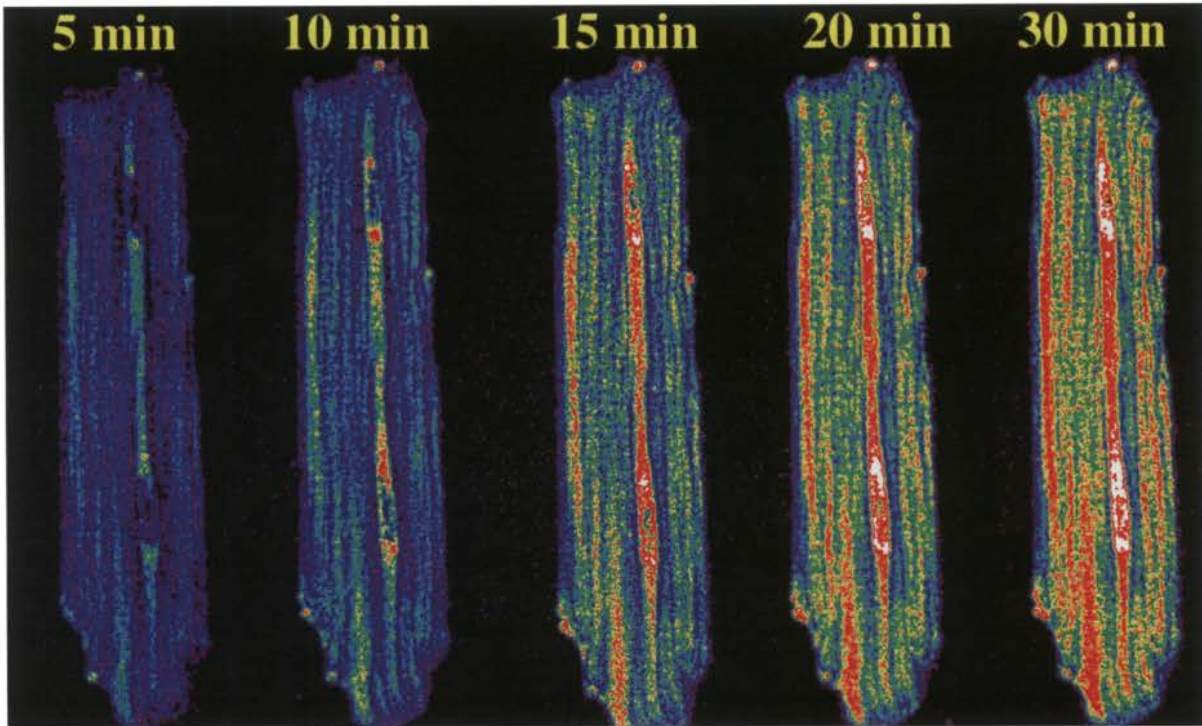
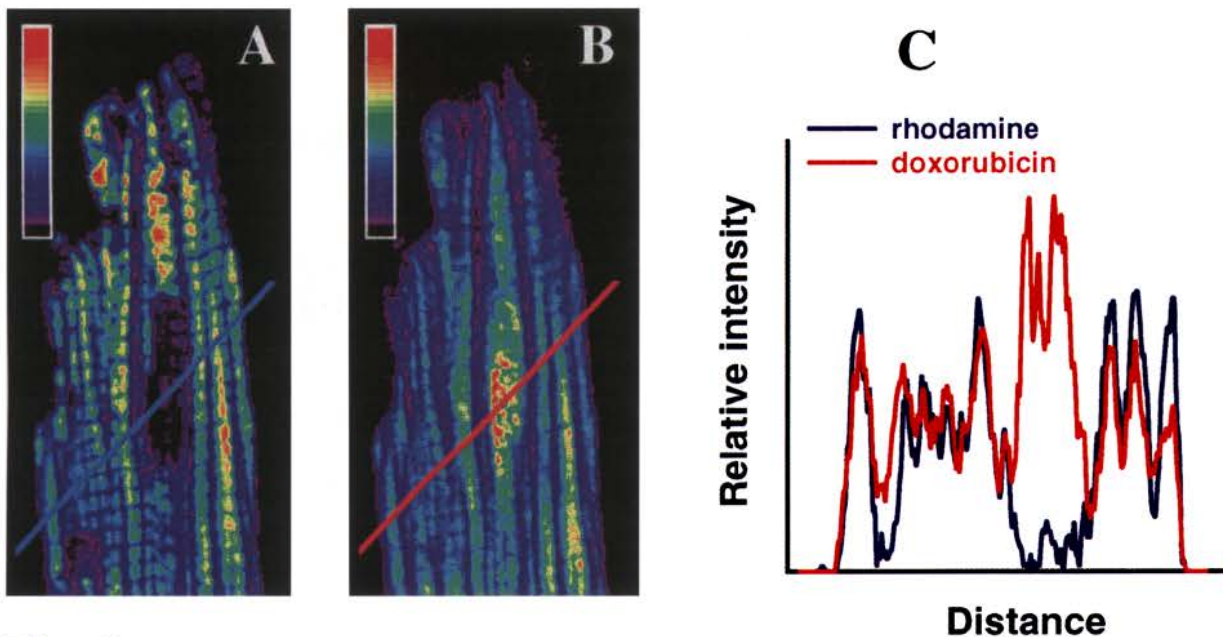


Fig. 1. Emission spectra of dichlorofluorescein and doxorubicin at 488-nm excitation. Vertical lines show emission ranges selected for *channels I* and *II*. Dashed line, dichlorofluorescein; solid line, doxorubicin.





**Fig.2.**



**Fig.3.**

Fig. 2. Time course of doxorubicin penetration into a myocyte. Color scale shows false color referring to increasing fluorescent values, from lowest (purple) to highest (white). Images were collected on *channel II* after 5, 10, 15, 20, and 30 min of incubation with 160  $\mu$ M doxorubicin.

Fig. 3. Dual staining of a cardiomyocyte with doxorubicin and rhodamine-123. *A*: rhodamine-123 characteristic staining seen in detection *channel I*. Spatial distribution of pixel intensities along diagonal line is presented in *C*. *B*: doxorubicin staining in detection *channel II*. Spatial distribution of pixel intensities along diagonal line is presented in *C*. *C*: line intensity profiles for doxorubicin and rhodamine coincide with correlation coefficient of  $0.94 \pm 0.03$ . Nuclear areas were excluded from correlation analysis.



and intracellular distribution of the drug during that period of time. Figure 2 illustrates sequential images of the same cell acquired at 5-min intervals after application of 160  $\mu\text{M}$  doxorubicin. Figure 2 shows rapid accumulation of the drug in the nucleus (myocytes are mostly binuclear cells) and subcellular organelles resembling mitochondrial pattern distribution.

**Dual staining with rhodamine-123 and doxorubicin.** To verify mitochondrial localization of the doxorubicin, myocytes were stained simultaneously with doxorubicin and rhodamine-123. Rhodamine-123 is a classic cationic mitochondrial marker that rapidly penetrates cell membranes (25). Rhodamine-123 exhibits maximum emission peak at 526 nm when excited at 488 nm; therefore, rhodamine-123 and doxorubicin fluorescence could be separated by detection on *channels I* and *II*, respectively (see MATERIALS AND METHODS). Figure 3 illustrates a myocyte stained simultaneously with both compounds: *A* shows rhodamine-123 distribution (*channel I*), and *B* shows doxorubicin staining (*channel II*). Line intensity profiles reveal a strong correlation between the spatial distributions of the compounds (Fig. 3C), with a correlation coefficient of  $0.94 \pm 0.03$  (the nuclear region was excluded from calculations). Therefore, data confirm mitochondrial localization of doxorubicin and provide information about the sites of increased oxidation caused by acute drug exposure (see below).

**Increase in intracellular oxidation associated with doxorubicin exposure.** For each cell preparation, control images (e.g., from control cells, cells preloaded with DFDA, and cells exposed to doxorubicin alone) were collected, averaged, and quantified. The level of fluorescence was undetectable for the control cells and very low for DFDA-loaded or doxorubicin-treated cells. Under exactly the same conditions and settings, a significant increase in dichlorofluorescein fluorescence intensity was observed on *channel I*, when DFDA-loaded cells had been exposed to doxorubicin for 20 min (Fig. 4). *A* and *B* present typical images of DFDA-loaded doxorubicin-exposed cells acquired on two channels simultaneously. Increase in dichlorofluorescein fluorescence was observed on *channel I* after 20 min of doxorubicin exposure. The increase in dichlorofluorescein fluorescence was highly reproducible and was observed in six different cell preparations, although the magnitude of the effect differed in cells isolated from different hearts, probably reflecting different antioxidant capacities of the individual hearts. Figure 4C shows the magnitude of the effect for different doxorubicin concentrations (myocytes from a single cell preparation were employed). The data reveal a concentration-dependent increase in the level of intracellular oxidation

associated with acute doxorubicin exposure. The most intense staining is found in cytosol surrounding mitochondria (the penetration of the dye inside the mitochondria and its subsequent oxidation are also conceivable). Because of cytosolic distribution of the probe, the areas corresponding to the nucleus remain dark (Fig. 4A). No prominent staining was observed close to the nucleus or plasma membrane.

**Long-term incubation of cardiomyocytes with low concentration of doxorubicin.** Numerous studies, including our own (23), have shown that 50–200  $\mu\text{M}$  doxorubicin causes formation of oxygen free radicals in heart cytosolic and mitochondrial preparations (3, 7, 8), yet clinically observed plasma concentrations are about two orders of magnitude lower (18). These facts challenge the occurrence of doxorubicin-associated oxidative stress *in vivo*; thus it was essential to estimate accumulated levels of the drug after exposure of cardiomyocytes to clinically relevant concentrations of the drug. Incubation of the myocytes with 1  $\mu\text{M}$  doxorubicin for 20 h leads to a significant accumulation of the drug (or its derivatives) inside the cells (Fig. 5). To quantify this effect, the fluorescence was calibrated with the set of buffers having specified doxorubicin concentrations (the fluorescence signal was detected from the same focal plane where the cells were found). Mean fluorescence intensity was calculated and used as an estimate of intracellular doxorubicin concentrations (Fig. 5C). As expected, the highest concentrations were observed in the nucleus. Evaluation of the nuclear levels of doxorubicin was not feasible, because fluorescence is quenched after drug intercalation into the DNA helix (1). Extranuclear levels of doxorubicin reached 25–50  $\mu\text{M}$  concentrations (which corresponds to the purple-blue color in Fig. 5), that were about two orders of magnitude higher than the extracellular concentration (because of differences in viscosity and intracellular environment, these values if anything will underestimate, rather than overestimate, the true intracellular concentration of the doxorubicin or its derivatives).

## DISCUSSION

In a previous study, doxorubicin, an anthracycline antitumor agent, was found to increase the cytosolic formation of superoxide anions and reduce the viability of cardiomyocytes with depleted levels of cytosolic superoxide dismutase (23). To monitor cellular localization of oxidative stress associated with doxorubicin exposure, the present study employs confocal microscopy with the oxidant-sensitive fluorescent probe DFDA. DFDA is a stable lipid-soluble compound that is readily taken up by the myocytes, deacetylated by cytosolic

Fig. 4. Effect of doxorubicin on oxidation of intracellular dichlorofluorescein. *A*: a typical fluorescence image seen on *channel I* when a DFDA-loaded myocyte was incubated with 80  $\mu\text{M}$  doxorubicin for 20 min. *B*: doxorubicin staining on *channel II* for myocyte in *A*. *C*: concentration-dependent effects of doxorubicin on mean fluorescence intensity on *channel I*. Values are means  $\pm$  SE;  $n = 7$  for DFDA-loaded cells and  $n = 4$  for control cells.

Fig. 5. Intracellular accumulation of doxorubicin after long-term exposure. *A*: whole cell image of a cardiac myocyte after 20 h of exposure to 1  $\mu\text{M}$  doxorubicin. *B*: enlarged image of myocyte showing distinct doxorubicin staining. *C*: doxorubicin calibration curve. Pixel intensity levels were assigned to each concentration on basis of mean fluorescence intensity of buffers with known doxorubicin concentrations. Color bar shows how pixel intensity corresponds with image color.



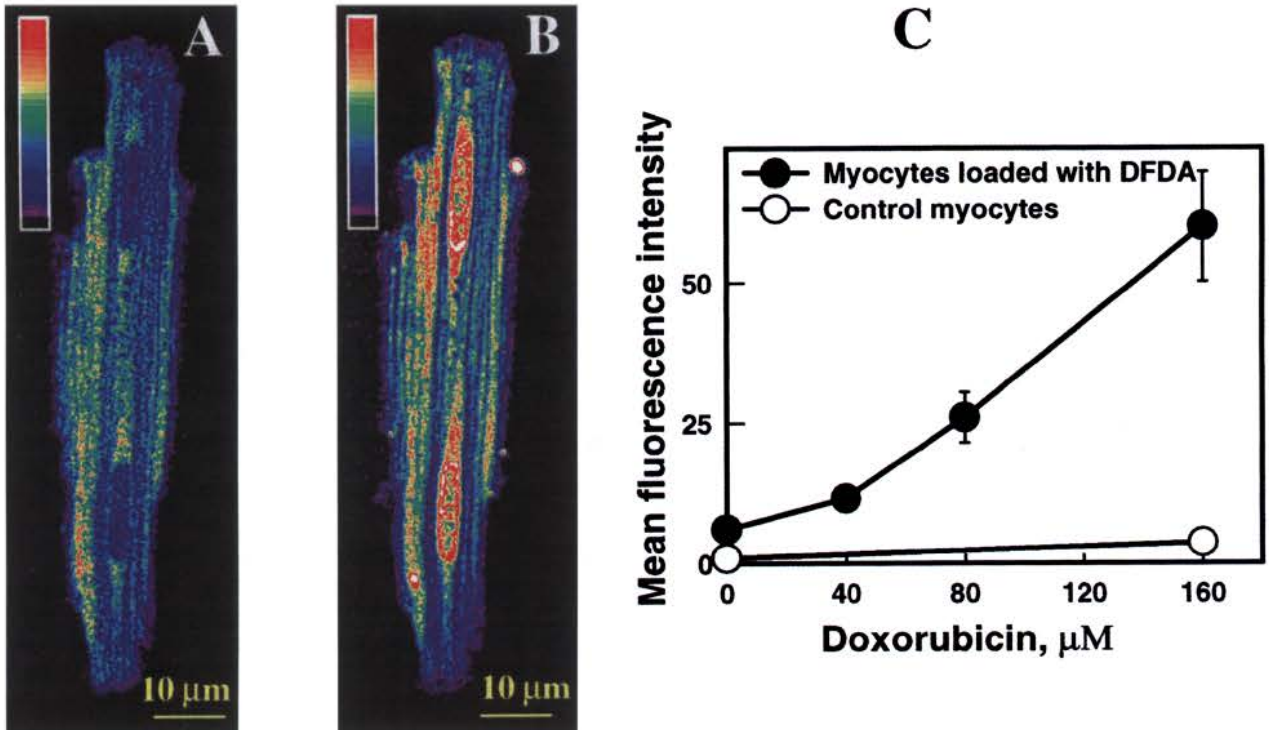


Fig.4.

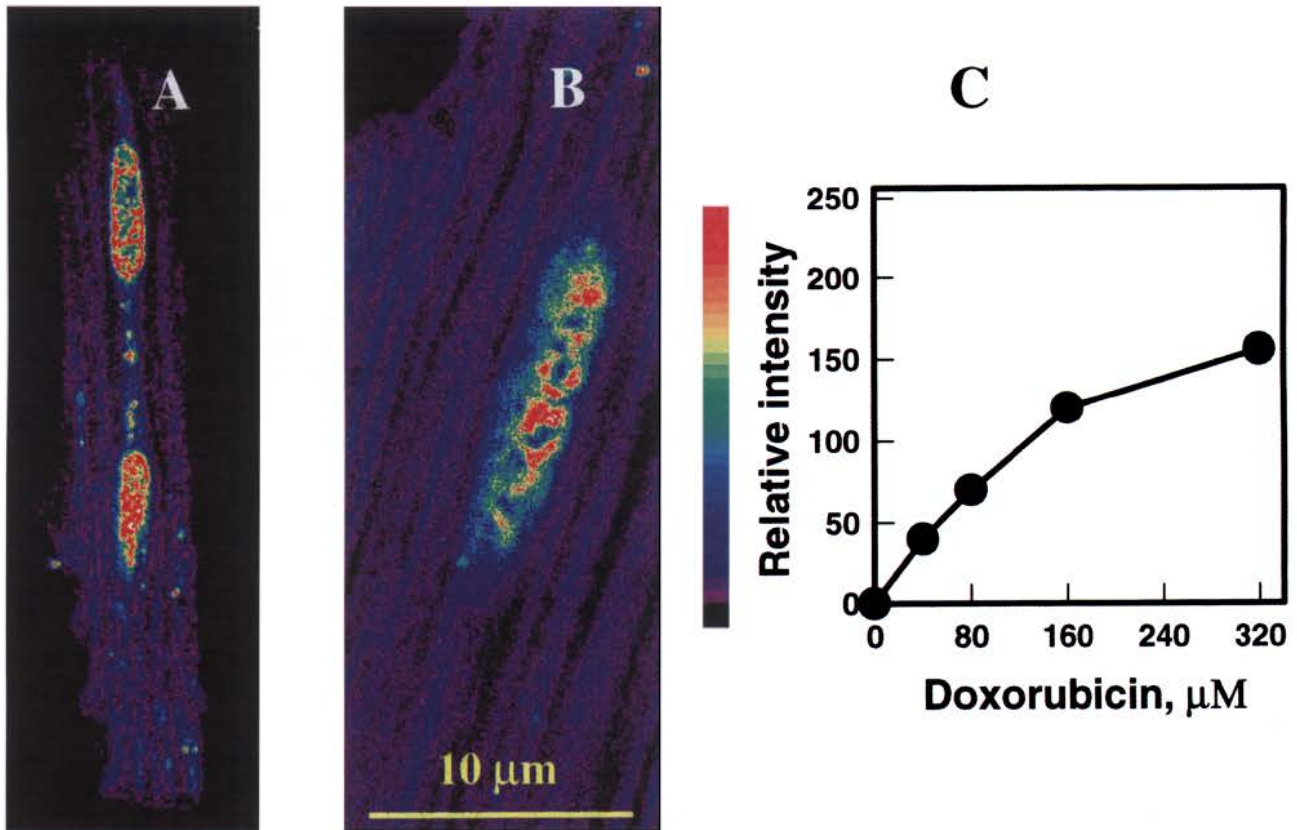


Fig.5.



enzymes into a nonfluorescent product, and trapped within the cytoplasm. Dichlorofluorescein is then oxidized to the highly fluorescent probe dichlorofluorescein. This transformation from the nonfluorescent to the fluorescent form is irreversible and reports cumulative oxidation (28).

The increase in dichlorofluorescein fluorescence observed in this study is consistent with the suggested oxidative mechanism of doxorubicin cardiotoxicity. It has been shown that, in the presence of NADH, doxorubicin can increase superoxide production in the cytosolic fraction of rat heart by >10-fold (7). However, this effect was inhibited by allopurinol and, therefore, could reflect the effect of xanthine oxidase released from endothelial cells, because this enzyme is negligible in cardiomyocytes (12). Another enzyme that could contribute to the observed increase in oxidation levels is sarcosomal NADPH:cytochrome *P*-450, because its activity has been shown to increase doxorubicin-mediated superoxide formation (7, 8).

The detected oxidation of dichlorofluorescein after acute doxorubicin exposure occurred close to the mitochondria (Fig. 4, *A* and *B*). The formation of reactive oxygen species by doxorubicin at the level of the mitochondria has been a subject of several studies (3, 4, 7, 8). It was attributed to cyclic reactions with doxorubicin semiquinone radicals (14, 18) and has been proposed to occur between complexes I and III of the mitochondrial respiratory chain (3). Another possibility is based on the strong correlation between oxidative stress and mitochondrial  $\text{Ca}^{2+}$ . Several studies suggest that doxorubicin-induced alterations in mitochondrial  $\text{Ca}^{2+}$  homeostasis increase the permeability of the inner mitochondrial membrane and lead to release of superoxide radical anions to the cytosolic face of the mitochondria (3, 5). However, this study suggests that an increase in oxidation due to doxorubicin exposure may precede changes in mitochondrial  $\text{Ca}^{2+}$ , because significantly elevated levels of oxidation were detected 20 min after exposure to the drug (Fig. 4C). A similar time course (15 min) for an increase in reactive oxygen species was noted when Chacon and Acosta (3) exposed isolated rat mitochondria to 50  $\mu\text{M}$  doxorubicin. In a separate study these authors showed, however, that a 3-h exposure of intact neonatal cardiac myocytes to 50  $\mu\text{M}$  doxorubicin was required for detection of changes in mitochondrial  $\text{Ca}^{2+}$  (4).

The oxidative stress observed in the present study was prominent after 20 min of the doxorubicin exposure. Therefore, an increase in intracellular oxidation apparently precedes changes in rod-shaped cell morphology and permeability of the cell to trypan blue, because, as shown in our earlier study (24), the latter changes become evident only when myocyte exposure to specified concentrations of the drug exceeds 40 min.

Although very high accumulation of the doxorubicin in the nucleus was observed (Fig. 2), it is unlikely that its diffusion from the nucleus affects cytosolic oxidation, because the semiquinone radical is relatively unstable, with an estimated diffusion radius of only 0.1  $\mu\text{m}$  under aerobic conditions (26). The present data also

do not support the idea that superoxide and hydrogen peroxide diffusing from the nucleus affect cytosolic oxidation, because no distinct increase in fluorescence was detected close to the nucleus (Fig. 4A).

The main argument against the free radical hypothesis of doxorubicin toxicity is that numerous studies on isolated cardiac preparations or subcellular organelles used doxorubicin concentrations significantly higher than those encountered in clinical practice (6, 7). However, even a 20-h incubation with doxorubicin (brief in comparison with the duration of clinical trials) leads to very high mitochondrial concentrations of the drug (Fig. 5), apparently because of the avid affinity of doxorubicin for cardiolipin (9). The accumulated drug concentrations were approximately two orders of magnitude higher than the original concentration of doxorubicin in the bathing medium, suggesting that formation of oxygen radical species observed in *in vitro* preparations (3, 7, 23) might also occur *in vivo*. Thus it is reasonable to suggest that the formation of oxygen free radicals is one component of chronic doxorubicin cardiotoxicity occurring concurrently with other factors, *i.e.*, drug-induced inhibition of topoisomerase II (15) and alterations of myosin isoform expression (10). However, the disturbances in protein synthesis are unlikely to explain the systolic and diastolic dysfunction that often occurs minutes after injection of anthracyclines (6). Such acute events could be caused, at least in part, by the rapid oxidative stress associated with doxorubicin treatment that was observed in this study.

In conclusion, this study presents direct evidence of an increase in intracellular oxidation associated with doxorubicin exposure of live cardiac myocytes. The images obtained using confocal laser-scanning microscopy reveal that significant levels of oxidation-sensitive fluorescence can be observed soon after drug penetration into the cell.

The author is very grateful to Dr. Richard Nathan for critical reading of the manuscript and for invaluable suggestions, Drs. Sandra Sabatini, Raul Martinez-Zaguilan, and Sandor Gyorke for helpful comments, and Charles Butterick for technical assistance.

This work was supported in part by a Seed Grant from Texas Tech University Health Sciences Center.

Address for reprint requests: N. Sarvazyan, Dept. of Physiology, Texas Tech University Health Sciences Center, 3601 4th St., Lubbock, TX 79430 (E-mail: phynas@ttuhsu.edu).

Received 30 January 1996; accepted in final form 5 April 1996.

## REFERENCES

1. Bachur, N., M. Gee, and R. Friedman. Nuclear catalyzed antibiotic free radical formation. *Cancer Res.* 42: 1078–1082, 1982.
2. Bondy, S. The relation of oxidative stress and hyperexcitation to neurological disease. *Proc. Soc. Exp. Biol. Med.* 208: 337–345, 1995.
3. Chacon, E., and D. Acosta. Mitochondrial regulation of superoxide by  $\text{Ca}^{2+}$ : an alternative mechanism for the cardiotoxicity of doxorubicin. *Toxicol. Appl. Pharmacol.* 107: 117–128, 1991.
4. Chacon, E., R. Ulrich, and D. Acosta. A digital-fluorescence imaging study of mitochondrial  $\text{Ca}^{++}$  increase by doxorubicin in cardiac myocytes. *Biochem. J.* 281: 871–878, 1992.
5. Crompton, M., and A. Costi. Kinetic evidence for a heart mitochondrial pore activated by  $\text{Ca}^{++}$ , inorganic phosphate and oxidative stress. *Eur. J. Biochem.* 178: 489–501, 1988.



6. **Ditchey, R., M. le Winter, and C. Higgins.** Acute effects of doxorubicin (adriamycin) on left ventricular function in dogs. *Int. J. Cardiol.* 16: 341–350, 1989.
7. **Doroshov, J.** Effect of anthracycline antibiotics on oxygen radical formation in rat heart. *Cancer Res.* 43: 460–472, 1983.
8. **Gervasi, P., M. Agrillo, A. Lippi, N. Bernardini, R. Danesi, and M. Del Tacca.** Superoxide anion production by doxorubicin analogs in heart sarcosomes and by mitochondrial NADH dehydrogenase. *Res. Commun. Chem. Pathol. Pharmacol.* 67: 101–115, 1990.
9. **Goormaghtigh, E., and J. Ruyschaert.** Anthracycline glycoside-membrane interaction. *Biochim. Biophys. Acta* 779: 271–288, 1984.
10. **Ito, H., S. Miller, M. Billingham, H. Alimoto, S. Torti, R. Wade, C. Gahlmann, G. Lyons, L. Kedes, and F. Torti.** Doxorubicin selectively inhibits muscle gene expression in cardiac muscle cells in vivo and in vitro. *Proc. Natl. Acad. Sci. USA* 87: 4275–4279, 1990.
11. **Jennings, R., and K. Reimer.** The cell biology of acute myocardial ischemia. *Annu. Rev. Med.* 42: 225–246, 1991.
12. **Jong, J. de, P. van der Meer, A. Nieukoop, T. Huizer, R. Stroeve, and E. Bos.** Xanthine oxidoreductase activity in reperfused hearts of various species, including human. *Circ. Res.* 67: 770–773, 1990.
13. **Juicher, R., A. van der Laarse, L. Sterrenberg, C. van Treslong, A. Bast, and J. Noordhoek.** The involvement of an oxidative mechanism in the adriamycin induced toxicity in neonatal rat heart cell cultures. *Res. Commun. Chem. Pathol. Pharmacol.* 47: 35–47, 1985.
14. **Keizer, H., H. Pinedo, G. Schuurhuis, and H. Joenje.** Doxorubicin (adriamycin): a critical review of free radical-dependent mechanisms of cytotoxicity. *Pharmacol. Ther.* 47: 219–231, 1990.
15. **Kreuser, E., S. Wadler, and E. Thiel.** Biochemical modulation of cytotoxic drugs by cytokines: molecular mechanisms in experimental oncology. *Recent Results Cancer Res.* 139: 371–382, 1995.
16. **Lown, J. W.** Anthracycline and anthraquinone anticancer agents: current status and recent developments. *Pharmacol. Ther.* 60: 185–214, 1993.
17. **Ogura, R., M. Sugiyama, H. Haramaki, and T. Hidaka.** Electron spin resonance studies on the mechanism of adriamycin-induced heart mitochondrial changes. *Cancer Res.* 51: 3555–3558, 1991.
18. **Olson, R., and P. Mushlin.** Doxorubicin cardiotoxicity: analysis of prevailing hypotheses. *FASEB J.* 4: 3076–3086, 1990.
19. **Pessan, I., E. Durie, M. Scheidt, and I. Zimanyi.** Anthraquinone-sensitized  $\text{Ca}^{2+}$  release channel from rat cardiac sarcoplasmic reticulum: possible receptor-mediated mechanism of doxorubicin cardiomyopathy. *Mol. Pharmacol.* 37: 503–514, 1990.
20. **Reynolds, I., and T. Hastings.** Glutamate induces the production of reactive oxygen species in cultured forebrain neurons following NMDA receptor activation. *J. Neurosci.* 15: 3318–3327, 1995.
21. **Rice-Evans, C., A. Diplock, and M. Symons.** *Techniques in Free Radical Research.* London: Elsevier, 1991.
22. **Royall, J., and H. Ischiropoulos.** Evaluation of 2',7'-dichlorofluorescein and dihydrorhodamine 123 as fluorescent probes for intracellular  $\text{H}_2\text{O}_2$  in cultured endothelial cells. *Arch. Biochem. Biophys.* 302: 348–355, 1993.
23. **Sarvazyan, N., A. Askari, and W.-H. Huang.** Effects of doxorubicin on cardiomyocytes with reduced levels of superoxide dismutase. *Life Sci.* 57: 1003–1010, 1995.
24. **Sarvazyan, N., A. Askari, L. Klevay, A. Askari, and W.-H. Huang.** Role of intracellular superoxide dismutase in oxidant-induced injury to normal and copper deficient cardiac myocytes. *Am. J. Physiol.* 268 (Heart Circ. Physiol. 37): H1115–H1121, 1995.
25. **Summerhayes, I., T. Lampidis, and S. Bernall.** Unusual retention of rhodamine 123 by mitochondria in muscle and carcinoma cells. *Proc. Natl. Acad. Sci. USA* 79: 5292–5296, 1982.
26. **Svingen, B., and G. Powis.** Pulse radiolysis studies of antitumor quinones: radical lifetimes, reactivity with oxygen and one-electron reduction potential. *Arch. Biochem. Biophys.* 209: 119–126, 1981.
27. **Ubesio, P., and F. Civoli.** Flow cytometric detection of hydrogen peroxide production induced by doxorubicin in cancer cells. *Free Radicals Biol. Med.* 16: 509–516, 1994.
28. **Zhu, H., G. Bannerberg, P. Moldeus, and H. Shertzer.** Oxidation pathways for the intracellular probe 2',7'-dichlorofluorescein. *Arch. Toxicol.* 68: 582–587, 1994.

